INTELLIGENT COMPUTATIONS FOR FLOOD MONITORING

Nataliia Kussul, Andrii Shelestov, Serhiy Skakun

Abstract: Floods represent the most devastating natural hazards in the world, affecting more people and causing more property damage than any other natural phenomena. One of the important problems associated with flood monitoring is flood extent extraction from satellite imagery, since it is impractical to acquire the flood area through field observations. This paper presents a method to flood extent extraction from synthetic-aperture radar (SAR) images that is based on intelligent computations. In particular, we apply artificial neural networks, self-organizing Kohonen's maps (SOMs), for SAR image segmentation and classification. We tested our approach to process data from three different satellite sensors: ERS-2/SAR (during flooding on Tisza river, Ukraine and Hungary, 2001), ENVISAT/ASAR WSM (Wide Swath Mode) and RADARSAT-1 (during flooding on Huaihe river, China, 2007). Obtained results showed the efficiency of our approach.

Keywords: flood extent extraction, neural networks, data fusion, SAR images.

ACM Classification Keywords: I.4.6 Segmentation - Pixel classification

Conference: The paper is selected from XIVth International Conference "Knowledge-Dialogue-Solution" KDS 2008, Varna, Bulgaria, June-July 2008

Introduction

Increasing numbers of natural disasters have demonstrated to the mankind the paramount importance of the natural hazards topic for the protection of the environment and the citizens. Climate change is likely to increase the intensity of rainstorms, river floods, and other extreme weather events. The dramatic floods of Central and Eastern Europe in summer 2002 and spring 2001 and 2006 emphasize the extreme in climatic variations. Floods are among the most devastating natural hazards in the world, affecting more people and causing more property damage than any other natural phenomena (Wood 2001). That is why; the problems of flood monitoring and flood risk assessment are among priority tasks in national satellite monitoring systems and international system of systems GEOSS (GEO Work Plan, 2007-2009).

Efficient monitoring and prediction of floods and risk management is impossible without the use of Earth Observation (EO) data from space. Satellite observations enable acquisition of data for large and hard-to-reach territories, as well as continuous measurements. One of the important problems associated with flood monitoring is flood extent extraction, since it is impractical to acquire the flood area through field observations. Flood extent can be used for hydraulic models to reconstruct what happened during the flood and determine what caused the water to go where it did, for damage assessment and risk management, and can benefit to rescuers during flooding (Corbley 1999).

The use of optical imagery for flood monitoring is limited by severe weather conditions, in particular presence of clouds. In turn, SAR (synthetic aperture radar) measurements from space are independent of daytime and weather conditions and can provide valuable information to monitoring of flood events. This is mainly due to the fact that smooth water surface provides no return to antenna in microwave spectrum and appears black in SAR imagery (Elachi 1988; Rees 2001).

As a rule, flood extent extraction procedure consists of the following steps: image calibration, geocoding, orthorectification using digital elevation model (DEM) and shadowing effects removal, filtration, thematic processing, testing and results verification. This paper proposes to use artificial neural networks (NN), in particular self-organizing Kohonen's maps (SOMs) (Haykin 1999; Kohonen 1995), for SAR image segmentation and classification. SOMs provide effective software tool for the visualization of high-dimensional data, automatically discover of statistically salient features of pattern vectors in data set, and can find clusters in training data pattern space which can be used to classify new patterns (Kohonen 1995). We applied our approach to the processing of data acquired from three different satellites: ERS-2/SAR (during flooding on Tisza river, Ukraine and Hungary, 2001), ENVISAT/ASAR WSM (Wide Swath Mode) and RADARSAT-1 (during flooding on Huaihe river, China, 2007).

Existing approaches to flood extent extraction

To this end different methods were proposed to flood extent extraction from satellite imagery. In European Space Agency (ESA) multi-temporal technique is used to flood extent extraction from SAR images (ESA Earth Watch, http://earth.esa.int/ew/floods). This technique uses SAR images of the same area taken on different dates (one image is acquired during flooding and the second one in “normal” conditions). The resulting multi-temporal image clearly reveals change in the Earth’s surface by the presence of colour in the image. This method has been implemented in ESA’s Grid Processing on Demand (G-POD, http://eogrid.esrin.esa.int). In (Cunjian et al. 2001), threshold segmentation algorithm is applied to flood extent extraction from RADARSAT-1 imagery. The value of threshold is chosen manually. In (Csornai et al.2004), SAR (from ESA’s ERS-2) and optical data (Landsat TM, IRS WIFS/LISS, NOAA AVHRR) are used for flood monitoring in Hungary in 2001. To derive flood extent from SAR imagery change detection technique is applied.

Though these methods are rather simple and quick (in computational terms), they posses some disadvantages: need of manual threshold selection and image segmentation, require expertise in visual interpretation of SAR images, require the use of complex models for speckle reduction, spatial connections between pixels are not concerned. To overcome these difficulties we propose neural network approach to flood extent extraction. Our approach is based on SAR image segmentation using self-organizing Kohonen maps and further image classification using additional information on water bodies derived from Landsat-7/ETM+ images and Corine Land Cover (for European countries).

Data sets description

We applied our approach to the processing of remote-sensing data acquired from three different satellites: ERS-2 (flooding on Tisza river on March 2001 (Fig. 1),

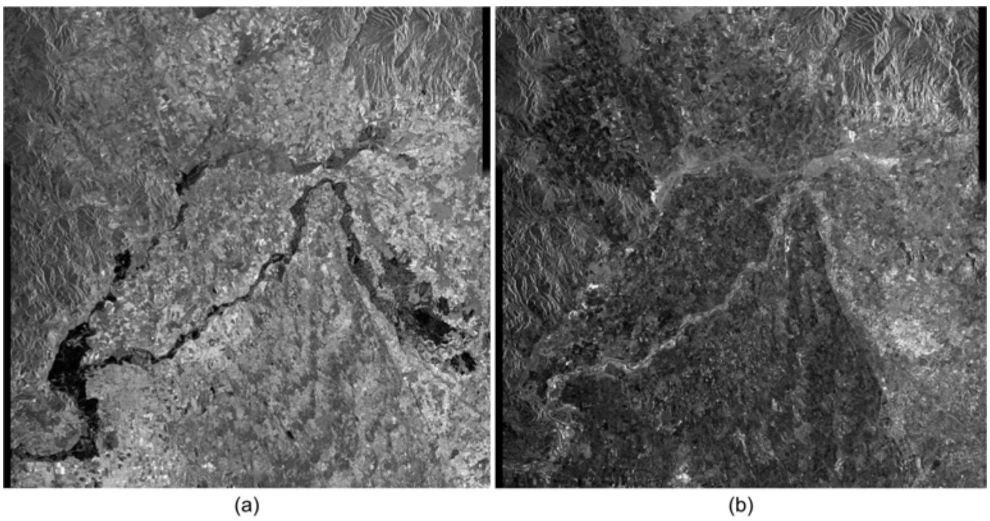

Fig. 1 Flooding (a, date of acquisition is 10.03.2001) and post-flooding (b, 14.04.2001) SAR/ERS-2 images of Tisza river (© ESA 2001)

ENVISAT and RADARSAT-1 (flooding on Huaihe river on July 2007 (Fig. 2). Data from European satellites were provided from ESA Category-1 project “Wide Area Grid Testbed for Flood Monitoring using Spaceborne SAR and Optical Data” (№4181). Data from RADARSAT-1 satellite were provided from RSGS-CAS. Spatial resolution of

ERS-2 images was 4 m (in ENVISAT SLC format (Single Look Complex)), for ENVISAT 75 m and for RADARSAT-1 was 12.5 m.

For more precise geocoding of SAR images and validation of obtained results we used the following set of additional data: Landsat-7/ETM+, European Corine Land Cover (CLC 2000) and SRTM DEM.

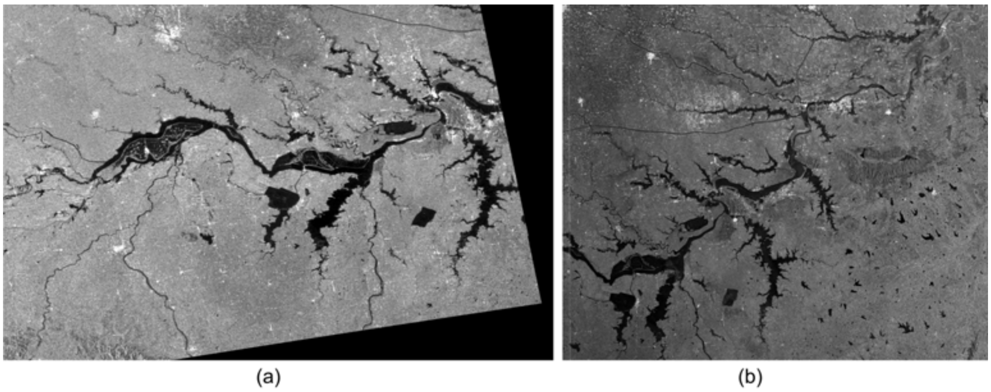

Fig. 2 SAR images acquired from ENVISAT (a, 15.07.2007) and RADARSAT-1 (b, 19.07.2007) satellites during flooding on Huaihe river, China (© ESA 2007; © CSA 2007)

In order to train and calibrate neural network, we manually chose test pixels (with the use of additional data set) that correspond to both territories with presence of water (we denote them as belonging to class "Water") and without water (class "No water"). The number of test pixels for each of the image is presented in Table 1.

Table 1. Distribution of test pixels for ERS-2, ENVISAT and RADARSAT-1 images

Satellite image/Region	Number of test pixels for images		
	"No water"	"Water"	Total
ERS-2/Ukraine	30016	12939	42955
ENVISAT/China	60575	34493	95068
RADARSAT-1/China	135263	130244	265507

Among test pixels we did not use those ones that relate to boundaries between water and no water lands. Classification of SAR images on more than two classes (e.g. "Water", "No water", different levels of water presence) is beyond the scope of this paper and will be investigated in future papers.

Neural network method for flood extent extraction from SAR imagery

Our method for flood extent extraction consists of data pre-processing, image segmentation and classification on two classes using SOMs. These steps are as follows:

1. *Transformation of raw data to lat/long projection*. Level-1 data from ERS-2 and ENVISAT satellites in Envisat format and from RADARSAT-1 satellite in CEOS format were provided with ground control points (GCPs) that were used to transform images to lat/long projection in GeoTIFF format. For this purpose, we used gdalwarp utility from GDAL (Geospatial Data Abstraction Library, http://www.gdal.org).

2. *Image calibration.* In order to calibrate ERS-2/SAR and ENVISAT/ASAR images, we used standard procedures described in (Laur et al. 2004) and (Rosich and Meadows 2004) respectively. As a result of image calibration, the output signal (pixel values) was transformed to backscatter coefficient (in dB). For RADARSAT-1 image, we used original pixel values in DN (digital number).

3. *Geocoding.* We made additional geocoding procedure for ERS-2 image in order to improve the accuracy. This was done by using Landsat/ETM+ and CLC2000 data.

4. *Image processing using self-organizing Kohonen's maps (SOMs)*. SOM is a type of artificial neural network that is trained using unsupervised learning to produce a low-dimensional (typically two dimensional), discretized representation of the input space of the training samples, called a map (Haykin 1999; Kohonen 1995). The map seeks to preserve the topological properties of the input space. SOM is formed of neurons located on a regular, usually 1- or 2-dimensional grid. Neurons compete with each other in order to pass to the excited state. The output of the map is a so called neuron-winner or best-matching unit (BMU) whose weight vector has the greatest similarity with the input sample x.

The network is trained in the following way: weight vectors $\mathbf{w}_j$ from topological neighbourhood of BMU vector i are updated according to (Haykin 1999; Kohonen 1995)

$$i(\mathbf{x}) = \arg\min_{j=\overline{1,L}} \left\| \mathbf{x} - \mathbf{w}_j \right\|,$$

$$\mathbf{w}_j(n+1) = \mathbf{w}_j(n) + \eta(n) h_{j,i(x)}(n)(\mathbf{x} - \mathbf{w}_j(n)), \quad j = \overline{1, L}, \qquad (1)$$

where η is learning rate, $h_{j,i(x)}(n)$ is neighborhood kernel around the winner unit *i*, x is input vector, $\|\cdot\|$ means Euclidean metric, *L* is number of neurons in the output grid, *n* is number of iteration within learning.

As neighborhood kernel $h_{j,i(x)}(n)$, we used Gaussian function. For learning rate we used the flowing expression:

$$\eta(n) = \eta_0 \cdot e^{-\frac{n}{\tau}}, \eta_0 = 0.1, n = 0,1,2,\ldots, \quad (2)$$

where τ is a constant.

Kohonen maps are widely applied to image processing, in particular image segmentation and classification (Haykin 1999). Before neural network training, we need to choose image parameters that will be input to neural network. For this purpose, one can choose original pixel values, various filters, Fourier transformation etc (Gonzalez and Woods 2002). In our approach we use sliding window with backscatter coefficient values for ERS-2 and ENVISAT images and DNs for RADARSAT-1 image as inputs to neural network. The output of neural network, neuron-winner, relates to the central pixel of sliding window. In order to choose appropriate size of the sliding window for each satellite sensor, we ran experiments for the following windows: 3-by-3, 5-by-5, 7-by-7, 9-by-9 and 11-by-11.

We, first, used SOM to segment each SAR image where each pixel of the output image was assigned a number of the neuron in the map. Then, we used test pixels to assign each neuron one of two classes ("Water" or "No water") using the following rule. If neuron was activated by majority number of pixels that belong to class "Water", then this neuron was assigned "Water" class. If neuron was activated by majority number of pixels that belong to class "No water", then this neuron was assigned "No water" class. If neuron was activated by neither of test pixels, then it was assigned "No data" class.

For neural network quality assessment, we used two parameters:

– quantization error that is estimated with the following expression

$$QE = \frac{1}{N} \sum_{t=1}^{N} \left\| \mathbf{x}_t - \mathbf{w}_{i(\mathbf{x}_t)} \right\|, \quad i(\mathbf{x}_t) = \arg\min_{j=\overline{1,L}} \left\| \mathbf{x}_t - \mathbf{w}_j \right\|,$$

where *N* is the number of test pixels.

– classification rate that shows relative number of correctly classified test pixels.

Results of image processing

In order to choose the best neural network architecture, we ran experiments for each image varying the following parameters:

- size of sliding window of images that define number of neurons in input layer of neural network;
- number of neurons in output layer, i.e. sizes of 2-dimensional output grid.

Other parameters that were used during image processing are as follows:

- neighborhood topology: hexagonal;
- neighborhood kernel around the winner unit: Gaussian function;
- initial learning rate: 0.1;
- number of training epochs: 20.

Initial values for the weight vectors are selected as a regular array of vectorial values that lie on the subspace spanned by the eigenvectors corresponding to the two largest principal components of input data (Kohonen 1995). Using this procedure, computation of the SOM can be made orders of magnitude faster, since (i) the SOM is then already approximately organized in the beginning, (ii) one can start with a narrower neighborhood function and smaller learning rate. The results of experiments for images are resented in Table 2.

For image with higher spatial resolution (ERS-2 and RADARSAT-1) the best results were achieved for larger input sliding window 7-by-7. In turn, for ENVISAT/ASAR WSM image we used sliding window of smaller size 3-by-3. The use of higher dimension of input window for ENVISAT image led to the coarser resolution of resulting flood extent image and reduced classification rate.

Table 2. Results of SAR images classification using SOMs

Satellite image	Input dimension	Output grid of neurons	Classification rate for test pixels		
			«No water»	«Water»	Total
ERS-2	7-by-7	5-by-5	99.81	99.86	99.90
ENVISAT	3-by-3	7-by-5	100.0	95.70	98.44
RADARSAT-1	7-by-7	5-by-5	99.99	91.92	96.03

The resulting flood extent images for ERS-2, ENVISAT and RADARSAT-1 satellite are shown on Fig. 3-5.

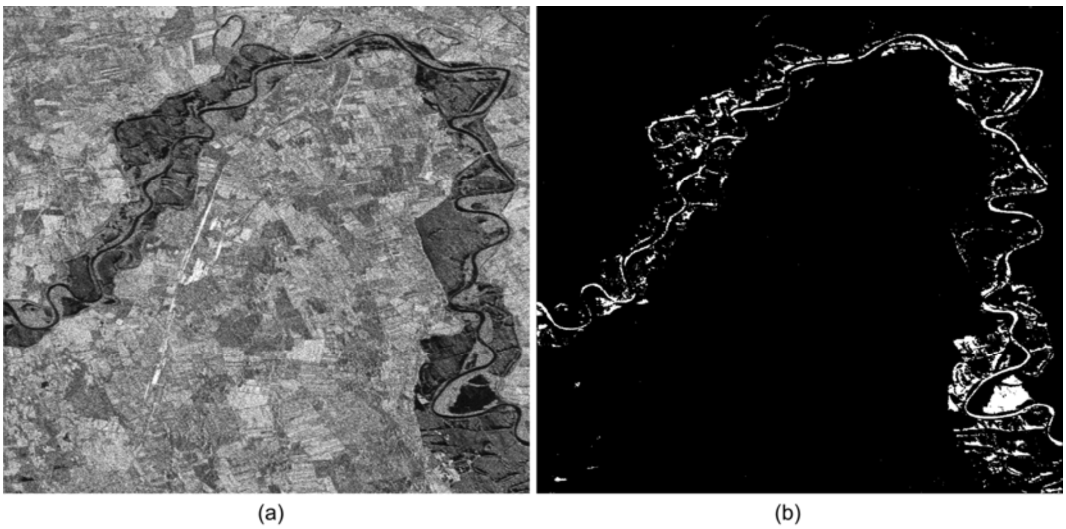

Fig. 3 Raw ERS-2 image (a) and resulting flood extent shown with white color (b) for Tisza river, Ukraine and Hungary (© ESA 2001)

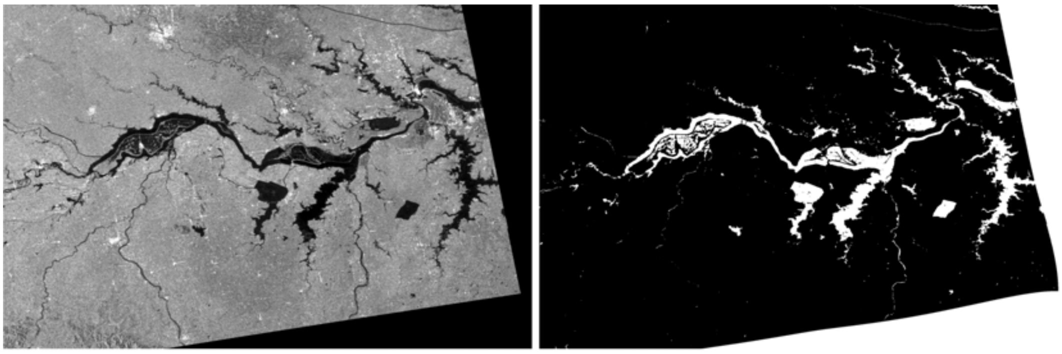

(a) (b)

Fig. 4 Raw ENVISAT image (a) and resulting flood extent shown with white color (b) for Huaihe river, China (© ESA 2007)

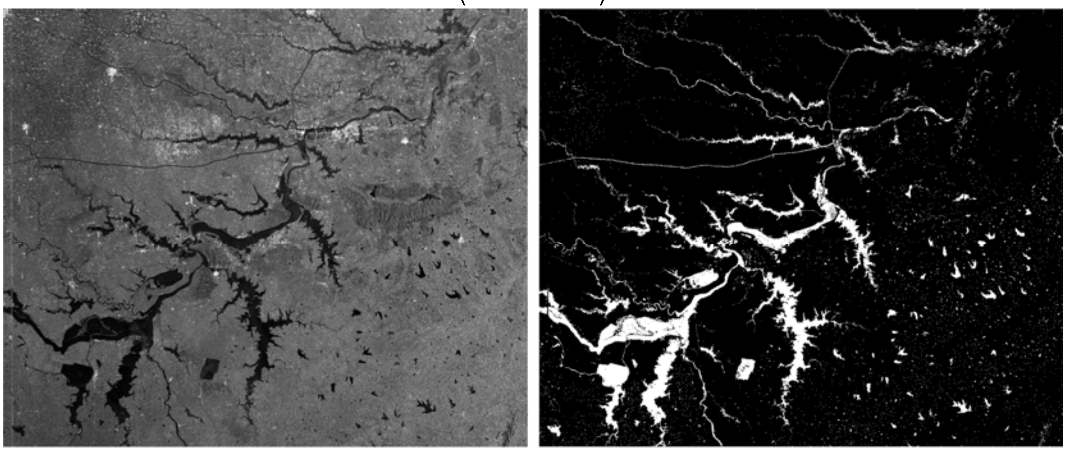

(a) (b)

Fig. 5 Raw RADARSAT-1 image (a) and resulting flood extent shown with white color (b) for Huaihe river, China (© CSA 2007)

Conclusions

In this paper we proposed neural network approach to flood extent extraction from SAR imagery. To segment and classify SAR image, we apply self-organizing Kohonen's maps (SOMs) that possess such useful properties as ability to automatically discover statistically salient features of pattern vectors in data set, and to find clusters in training data pattern space which can be used to classify new patterns. As inputs to neuron network, we use a sliding window of image pixels intensities. We ran experiments to choose the best neuron network architecture for each satellite sensor: for ERS-2 and RADARSAT-1 the size of input was 7-by-7 and for ENVISAT/ASAR the sliding window was 3-by-3. The advantages of our approach are as follows: (i) we apply sliding window to process the image and thus considering spatial connection between pixels; (ii) neural network's weight vectors are adjusted automatically by using training data. This enables implementation of our approach in automatic services for flood monitoring. Considering the selection of test pixels to calibrate the neuron network, i.e. to assign each neuron one of the classes, this process can be also automated using geo-referenced information on water bodies for the given region.

We applied our approach to derive flood extent from SAR images acquired by three different sensors: ERS-2/SAR for Tisza river (Ukraine); ENVISAT/ASAR and RADARSAT-1 for Huaihe river (China). Classification rates for manually selected test pixels were 99.99%, 91.92% and 96.03%, respectively. These results demonstrate the efficiency of our approach.

Acknowledgements

This work is supported by ESA CAT-1 project “Wide Area Grid Testbed for Flood Monitoring using Spaceborne SAR and Optical Data” (No. 4181) and by joint INTAS-CNES-NSAU project “Data Fusion Grid Infrastructure” (Ref. Nr 06-1000024-9154).

Bibliography

[Corbley, 1999] Corbley K.P. Radar Imagery Proves Valuable in Managing and Analyzing Floods Red River flood demonstrates operational capabilities. Earth Observation Magazine, 1999, vol. 8, num. 10.

[Csornai et al., 2004] Csornai G., Suba Zs., Nádor G., László I., Csekő Á., Wirnhardt Cs., Tikász L., Martinovich L. Evaluation of a remote sensing based regional flood/waterlog and drought monitoring model utilising multi-source satellite data set including ENVISAT data. In: Proc. of the 2004 ENVISAT & ERS Symposium (Salzburg, Austria, 6-10 September 2004).

[Cunjian et al., 2001] Cunjian Y., Yiming W., Siyuan W., Zengxiang Z., Shifeng H. Extracting the flood extent from satellite SAR image with thesupport of topographic data. In: Proc. of Int. Conf. on Inf. Tech. and Inf. Networks (ICII 2001), vol. 1, pp 87-92.

[Elachi,1988] Elachi C. Spaceborne Radar Remote Sensing: Applications and Techniques. New York: IEEE Press, 1988.

[Haykin, 1999] Haykin S. Neural Networks: A Comprehensive Foundation. Upper Saddle River, New Jersey: Prentice Hall, 1999.

[GEO Work Plan, 2007] GEO Work Plan 2007-2009 “Toward Convergence”. (www.earthobservations.org/documents/wp0709_v4.pdf)

[Gonzalez and Woods, 2002] Gonzalez R.C., Woods R.E. Digital Image Processing. Prentice Hall, Upper Saddle River, New Jersey, 2002.

[Kohonen, 1995] Kohonen T. Self-Organizing Maps. Series in Information Sciences, Vol. 30. Springer, Heidelberg, 1995.

[Laur et al., 2004] Laur H., Bally P., Meadows P., Sanchez J., Schaettler B., Lopinto E., Esteban D. ERS SAR Calibration. Derivation of the Backscattering Coefficient in ESA ERS SAR PRI Products. ES-TN-RS-PM-HL09 05, November 2004, Issue 2, Rev. 5f

[Rosich and Meadows, 2004] Rosich B., Meadows P. Absolute calibration of ASAR level 1 products generated with PF-ASAR. ESA-ESRIN, ENVI-CLVL-EOPG-TN-03-0010, 07 October 2004.

[Wood, 2001] Wood H.M. The Use of Earth Observing Satellites for Hazard Support: Assessments & Scenarios. Final Report. National Oceanic & Atmospheric Administration, Dep. of Commerce, USA, 2001. (http://www.ceos.org/pages/DMSG/2001Ceos/overview.html)

[Rees, 2001] Rees W.G. Physical Principles of Remote Sensing. Cambridge University Press, 2001.

Authors' Information

Nataliia Kussul – Prof., Dr., Head of Department of Space Information Technologies and Systems, Space Research Institute of NASU-NSAU, Glushkov Ave 40, build. 4/1, Kyiv-187, 03680 Ukraine, e-mail: inform@ikd.kiev.ua

Andrii Yu. Shelestov – PhD, Senior Researcher, Department of Space Information Technologies and Systems, Space Research Institute of NASU-NSAU, Glushkov Ave 40, build. 4/1, Kyiv-187, 03680 Ukraine, e-mail: inform@ikd.kiev.ua

Serhiy V. Skakun – PhD, Research Assistant, Department of Space Information Technologies and Systems, Space Research Institute of NASU-NSAU, Glushkov Ave 40, build. 4/1, Kyiv-187, 03680 Ukraine, e-mail: serhiy.skakun@ikd.kiev.ua